Laser and Particle Beams

cambridge.org/lpb

Experimental research on ultrasound-assisted underwater femtosecond laser drilling

Xiaoyan Sun, Jianhang Zhou, Ji-An Duan, Haifeng Du, Dongmei Cui and Youwang Hu

The State Key Laboratory of High Performance Complex Manufacturing, College of Mechanical and Electrical Engineering, Central South University, 932 South Lushan Street, Changsha, 410083, China

Research Article

Cite this article: Sun X, Zhou J, Duan J-A, Du H, Cui D, Hu Y (2018). Experimental research on ultrasound-assisted underwater femtosecond laser drilling. *Laser and Particle Beams* **36**, 487–493. https://doi.org/10.1017/S0263034618000538

Received: 11 October 2018
Revised: 15 November 2018
Accepted: 27 November 2018

Key words:
Femtosecond pulsed laser; laser ablation; laser micro-fabrication

Author for correspondence: Youwang Hu, The State Key Laboratory of High Performance Complex Manufacturing, College of Mechanical and Electrical Engineering, Central South University, 932 South Lushan Street, Changsha, 410083, China. E-mail: huyw@csu.edu.cn

Abstract

In order to diminish the occurrence of cavitation bubbles during the liquid-assisted laser machining, ultrasound-assisted underwater femtosecond laser drilling on stainless steel is adopted. This method greatly diminishes the optical disturbance of cavitation bubbles. By investigating and analyzing the effect of laser pulse energy and pulse number on the morphology of the holes, it has been found that ultrasound not only has a remarkable function of forming a hole with clean and flat bottom, but also reduces debris redeposition around the processing area. This method improves the machining quality. Besides, it also improves the depth-to-diameter ratio of the hole about 20%.

Introduction

With the development of laser technology, especially of the ultra-short pulse laser technology, laser micro-fabrication has been applied in different fields (Kawata *et al.*, 2001; Sun *et al.*, 2015; Chu *et al.*, 2017; Yin *et al.*, 2017; Zeng *et al.*, 2017). An ultra-short pulse laser is a laser that emits ultra-short pulses of light, generally of the order of femtoseconds to ten picoseconds. The mechanism of long pulse laser removal machining is thermal ablation, because it takes place on timescales much longer than 10^{-12} s, which is the energy relaxation time of the lattice. On the contrary, high intensity femtosecond pulse laser, ultrafast phase transition and ablation can occur before thermal process begins (Chichkov *et al.*, 1996; Zhu *et al.*, 2005). Hence, the thermal effect on the workpiece surface is obvious in picosecond laser and other long pulse laser machining (Chu *et al.*, 2017), whereas the femtosecond laser significantly reduces the thermal effect, greatly weakens the influence of material melting and resolidification (Matsumura *et al.*, 2005; Wang *et al.*, 2017).

Despite the aforementioned advantages, debris deposition, heat-affected zone (HAZ), and other thermally induced detrimental effects can't be ignored in femtosecond laser machining (Chien and Hou, 2007; Charee *et al.*, 2016; Deng *et al.*, 2016). Therefore, vacuum-assisted (Juodkazis *et al.*, 2004) and some water-assisted laser ablation technologies are proposed to reduce the negative influence, such as under water, water spray, over-flow, and thin water film (Liu *et al.*, 2016). During the laser ablation underwater process, water can reduce the size of HAZ and weaken the redeposition of removed material (Liu *et al.*, 2012; Nguyen *et al.*, 2014; Hu *et al.*, 2017). However, the material as well as the water surrounding the ablation region vaporize rapidly. It results in forming some expanding cavitation bubbles near the top of the laser irradiated area (Chen *et al.*, 2004; Abreu *et al.*, 2005; Tamura *et al.*, 2013).

The constant and unpredictable expansion and decay of the bubbles dynamically change the refraction and scattering of the laser beam underwater during the ablation. The serious consequence is that the actual laser intensity is weaker than that of the laser without bubbles. Meanwhile, the intensity of the light field of the laser focal point is always changing, and its distribution is not uniform (Tomko *et al.*, 2017). These optical disturbances are not acceptable for precise laser machining.

The ablated surface morphology and machining performance depend on the bubble size, so eliminating the bubble or reducing the bubble size is helpful to improve the machining quality (Zhang *et al.*, 2016). The size of cavitation bubble depends on many factors, such as water layer thickness, water temperature, and water speed. Besides, properties of the additives in water, surface characteristics of the workpiece and the focal position of the laser beam with respect to the workpiece surface can also affect the bubble size (Lauterborn and Bolle, 2006). However, attempts to reduce the size of bubbles drastically by altering these factors are not ideal. The water-assisted laser technologies mentioned above have also tried to diminish the effect of bubbles. However, the water spray technology can only be used in the minimum area of laser irradiation. The over-flow technology is not only difficult to build the experimental platform, but also can't guarantee the uniformity of water flow velocity on all parts of the sample, which reduces the processing quality. Wu (2014) proposed the ultrasound-assisted underwater

CAMBRIDGE UNIVERSITY PRESS

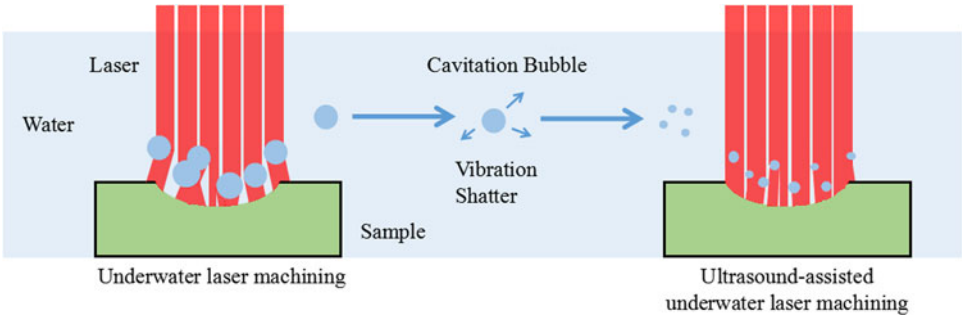

Fig. 1. Schematic diagram shows the mechanism of vibration shatters cavitation bubble to improve the quality of laser machining.

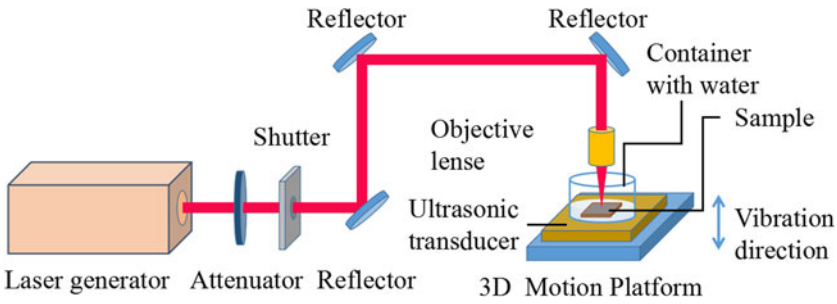

Fig. 2. Schematic diagram shows the setup of the experiment of ultrasound-assisted underwater femtosecond laser machining system.

laser machining, and the investigation in nano-pulse laser machining was done by Liu *et al.* (2014). The high frequency vibration caused by ultrasound assistance can obviously break up the cavitation bubbles into smaller ones, and the disturbance caused by bubbles to the laser beam is reduced. The mechanism of this method is shown in Figure 1.

As for the existing experiments which mainly study ultrasound-assisted laser machining in air and ultrasound-assisted underwater machining with long pulse laser, a common problem is that the re-deposition of clustered nanoparticles still changes the morphology of the holes. Therefore, we use the ultra-short pulse laser, combine underwater environment, and ultrasound assistance to solve this problem and describe the method in this paper.

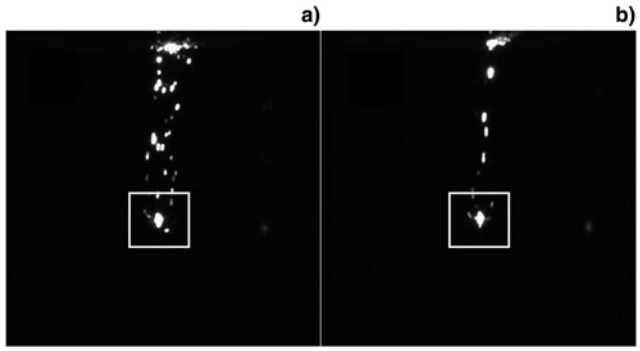

Fig. 3. Snapshot images of the femtosecond laser focal point underwater without (a) and with (b) ultrasound assistance.

Experimental methods

The schematic diagram shows the setup of the experiment of the ultrasound-assisted underwater femtosecond laser machining system (Fig. 2). A commercial Ti:sapphire femtosecond laser generator (Spectra Physics, Inc.) is used, generating horizontal linearly polarized laser pulses ($\tau = 120$ fs, $\lambda = 800$ nm center wavelength, $f = 1$ kHz pulse repetition frequency). The beam is focused onto the underwater samples by a 10× objective lens with a numerical aperture of 0.25. The surface of the water is 1 mm above the sample's surface. And the container with water is placed on the ultrasonic transducer (JP-520, frequency: 20 kHz, power: 15 W, vibration amplitude: 0.5 μm) which is fixed horizontally and can only vibrate in the vertical direction.

The laser drilling is performed on 2 mm thickness AISI 304 austenitic stainless steel. The surfaces of the steel specimens are polished to $R_a = 0.1$ μm. The pulse energies used in the experiments are 20, 40, 60, 80, and 100 μJ. For each energy, holes are produced by different pulse numbers ($N = 50$, 100, 200, and 500) with the replication of five. The diameter and depth of the hole are measured by a high magnification laser scanning confocal microscope (LSCM, Zeiss Axio LSM700, Germany). The machining morphology including cracks and debris deposition is also observed by a scanning electron microscope (SEM).

Results and discussion

Figure 3 shows the snapshot images of the femtosecond laser focal point underwater without (a) and with (b) ultrasound assistance taken by a complementary metal oxide semiconductor (CMOS, IU500M) camera. The points in the box are the focal points. Since the refractive index of air is less than water, bubbles underwater look brighter than water. In Figure 3b, it can be seen that the visible large bubbles are slightly smaller in size and significantly fewer in number than the left's, which verifies that the ultrasonic vibration can break the large cavitation bubbles generated by underwater laser machining.

Figure 4 shows the LSCM images of holes drilled by the femtosecond laser in air (a), underwater without (b), and with (c)

https://doi.org/10.1017/S0263034618000538 Published online by Cambridge University Press

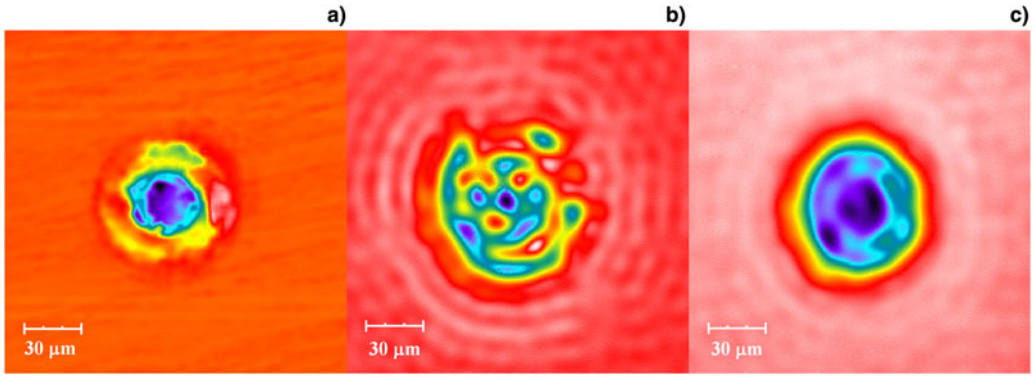

Fig. 4. LSCM images of holes drilled by the laser in air (a), underwater without (b), and with (c) ultrasound, using 500 pulses with the energy of 40 μJ.

ultrasound assistance. It can be roughly seen that the crater shape of the hole drilled in air is irregular, whereas the hole drilled in the water is larger and more rounded. The color distribution in the figure with ultrasound assistance is more uniform, which suggests that the change in the height of the hole bottom is small and the hole machining quality is better than the formers' machining.

In order to record the drilling process, the SEM images of holes drilled by the femtosecond laser underwater without (the left column) and with (the right column) ultrasound assistance are shown in Figure 5. The pulse energy is 100 μJ, and the pulse numbers are 50, 100, 200, and 500, respectively.

Comparing two columns in Figure 5, it shows that the diameter of the hole at 50 pulses is slightly smaller than those at 500 pulses, and the depth of the holes increases significantly with the increase of pulse number. However, the situation is different between the hole morphologies produced by femtosecond laser drilling with and without ultrasound assistance. In Vorobyev and Guo (2007) drilling experiment with femtosecond laser on titanium, they found that with higher pulse numbers and higher energy, the hole's structure would move from a nanometer scale to a micron scale. It can be seen that the morphology of the hole bottom in the left column becomes uneven, and the structure of nanometer scale appears from 50 pulses to 500 pulses. However, under the same number of laser pulses, hole bottoms in the right column are obviously more flat than those in the left that drilled without ultrasound assistance. This is consistent with the profiles measured by confocal microscopy shown in Figure 4. Meanwhile, in the right column, we observe that the non-target processing area around the crater has almost no trace of laser processing, the debris and splash of the crater are obviously less than the left. This is because the slight vibration of water caused by the ultrasonic vibration takes away the splashing debris during processing. At the same time, the less bubbles hardly produce laser scattering during processing, which also ensures the quality of processing.

In order to investigate the influence of ultrasound on the three-dimensional (3D) machining topography more prudently, the SEM images of holes with 500 pulse number and 40 μJ pulse energy are exhibited in Figure 6. Local amplified images are also shown there. The two columns are without ultrasound (left) and with ultrasound (right) assistance, respectively. Comparing the images in Figure 6a and 6b, it can be seen that the 3D machining profile of the hole drilled with ultrasound assistance is more regular than that drilled without ultrasound assistance. The bottom of the right hole looks like a plane, on the contrary, the left hole bottom is rugged and uneven. Figure 6c and 6d show the higher magnification SEM images of the central region at the bottom of the holes. It can be seen that many nanodroplets are uniformly formed at the bottom of the right hole. This is attributed to the introduction of ultrasound vibration, the movement of water and debris is more efficient due to local convection, the evaporated material is more likely to escape from the processing area. As a result, the ablated particles have less tendency to agglomerate (Park *et al.*, 2012; Yin *et al.*, 2016). While in the bottom of the left hole drilled without ultrasound, there are some rugged hills and a few small holes due to the resolidification of molten material without ejection. Figure 6e and 6f show the region of the crater of the hole at a higher magnification with ultrasound and without ultrasound assistance, respectively. Due to the refraction and scattering of the laser beam dynamically changed by the cavitation bubbles, left crater morphology obviously changed more irregular, rough and blurred, while the right's morphology is smoother as the cavitation bubbles are broken into smaller pieces by ultrasound vibration, and the disturbance caused by bubbles to the laser beam is reduced.

Figure 7 shows the two-dimensional (2D) profiles of holes drilled by 50, 100, 200, and 500 pulses, respectively, using two different machining methods with the energy of 100 μJ. The profiles are measured using a confocal microscope. It can be seen that as the number of pulses increases from 50 to 500, the hole depth of non-ultrasound-assisted and ultrasound-assisted femtosecond laser underwater drilling increases linearly. It can be seen that the morphology of the hole bottom drilled with ultrasound assistance is better than that without ultrasound assistance from the coordinate data on the Z axis.

Figure 8 shows the change trend of the hole depth with the pulse energy. It is obviously that the depth of the hole drilled by ultrasound-assisted femtosecond laser underwater machining is about 10–48% greater than that of non-ultrasound-assisted. Considering that the ultrasonic vibration frequency is much higher than the laser pulse frequency and the weak amplitude of the ultrasound, the vibration of the sample does not change the focus position significantly. In addition, the hole depth of two types of machining methods both show a tendency that increasing first and then decreasing with the increase of energy. When the laser pulse number is 50, the holes depth drilled with ultrasound assistance starts to decline with 80 μJ, whereas the hole depth drilled without ultrasound assistance starts to decline with 60 μJ. This experimental result is similar to the characteristic of the plasma shielding effect proposed Singh (1996) and Zeng *et al.* (2005). A high temperature highly ionized plasma is formed when the laser ablated material itself absorbs the laser beam. Due

https://doi.org/10.1017/S0263034618000538 Published online by Cambridge University Press

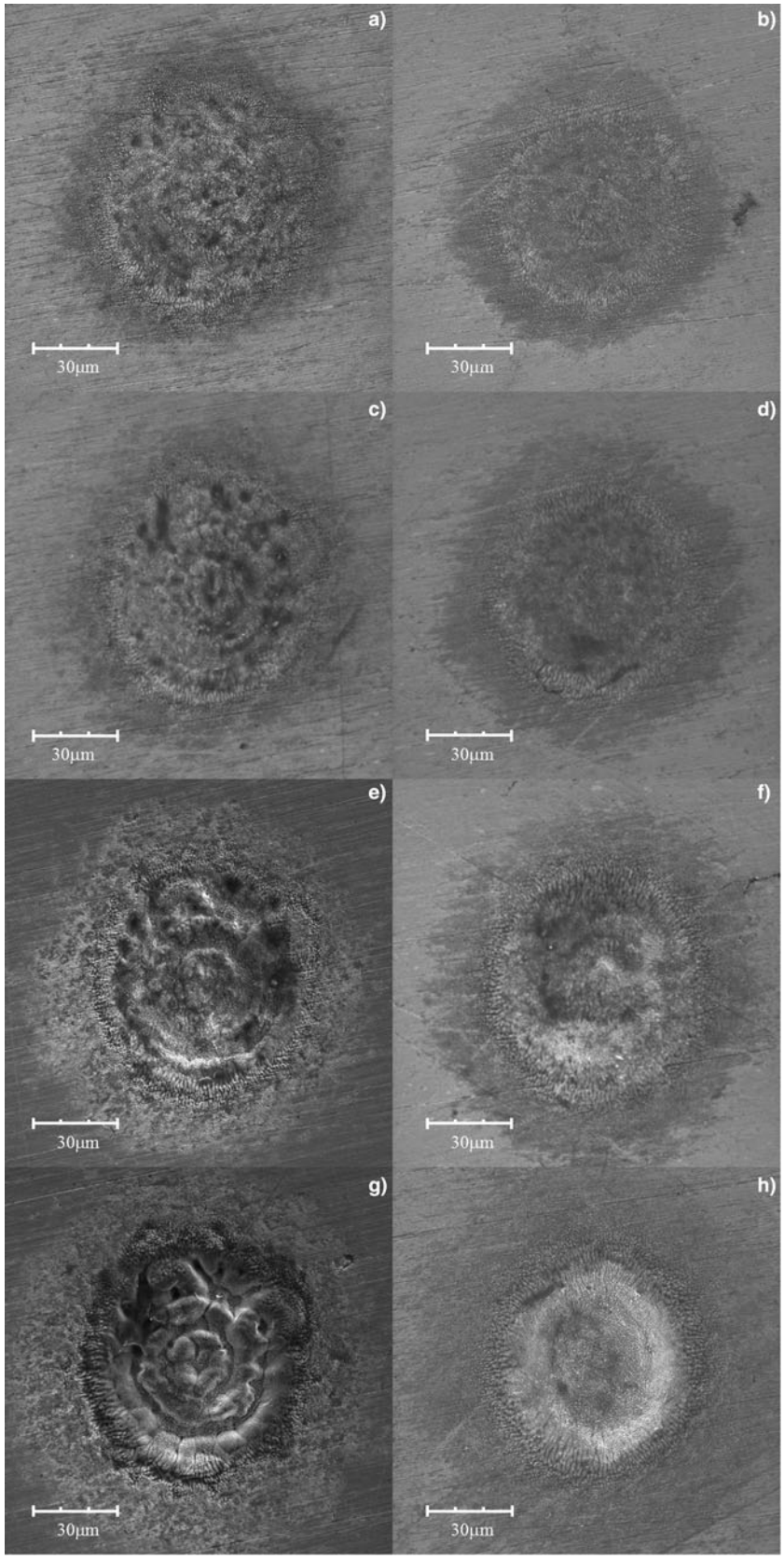

Fig. 5. SEM images of holes drilled by the laser underwater without (left) and with (right) ultrasound, using 50 (a, b), 100 (c, d), 200 (e, f), and 500 (g, h) pulses with the energy of 100 μJ.

to the laser fluence, the degree of plasma absorption can vary from 0% to nearly 100% of the incident laser energy. With the increase of the pulse energy, especially when the energy is higher than about 60 μJ, the plasma shielding effect is enhanced, and the holes depth shows the tendency to decrease after increase. The plasma shielding time depends on plasma spatial distribution

https://doi.org/10.1017/S0263034618000538 Published online by Cambridge University Press

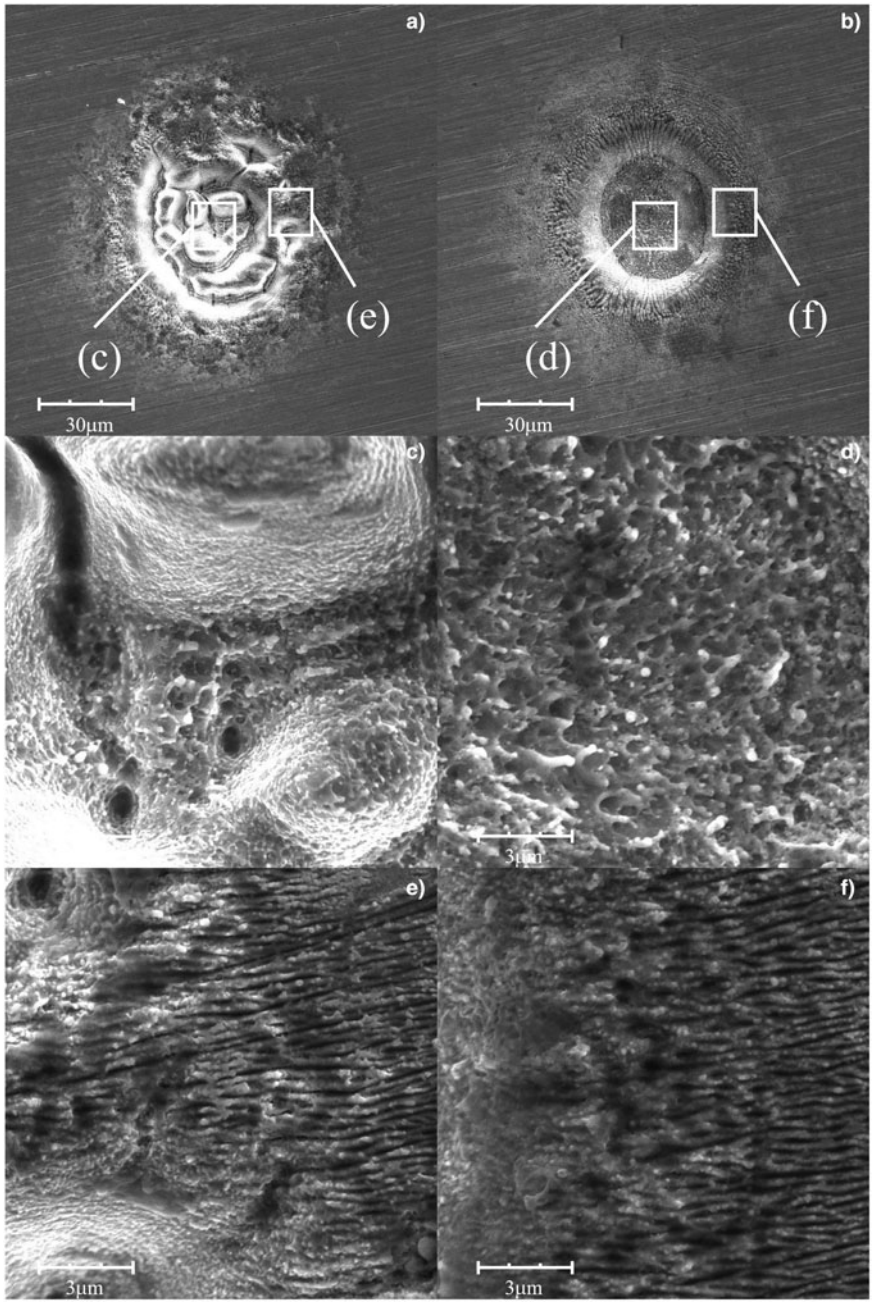

Fig. 6. SEM images of holes drilled by the laser underwater without (a) and with (b) ultrasound assistance, using 500 pulses with the energy of 40 μJ. Panels (c, e) and (d, f) show the SEM images of selected areas registered at a higher magnification in two different processing methods, respectively.

and electron density. Therefore, it has been found that the ultrasound vibration causes a reduction in plasma density and the holes drilled without ultrasound assistance are more likely to have plasma shielding for it tends to decrease earlier.

Figure 9 shows the diameter of holes as function of the pulse energy with two types of machining methods using four different pulse numbers. All of these holes diameter quickly increase with rising pulse energy in the range from 20 to 100 μJ. We find that under the same experimental conditions, the diameter of the holes drilled with ultrasound assistance is smaller than those non-ultrasound-assisted. The reason is that the cavitation bubbles generated in the water distort the laser beam, expand the ablation region, while the ultrasound vibration shatters the bubbles.

Figure 10 shows the depth-to-diameter ratio of holes in the function of the laser pulse energy with two types of machining methods, using four different pulse numbers. It can be seen that as the number of pulses increases from 50 to 500, the aspect ratio of non-ultrasound-assisted and ultrasound-assisted femtosecond laser underwater drilling increases linearly, while the aspect ratio is hardly affected by the change in energy. In addition, ultrasound-assisted underwater drilling can improve the depth to diameter ratio about 20%.

Conclusions

In summary, ultrasound-assisted femtosecond laser underwater drilling has been studied, under the investigated conditions using 50–500 pulses and 20–100 μJ energy. It is found that with ultrasound assistance, there is no obvious slag splash, burrs, and removed material redeposition on the workpiece surface.

https://doi.org/10.1017/S0263034618000538 Published online by Cambridge University Press

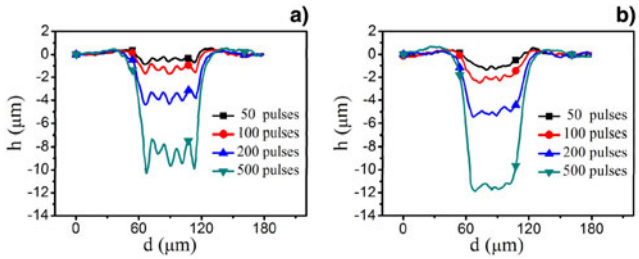

Fig. 7. Measured 2D profiles of the holes drilled on stainless steel without ultrasound (left) and with ultrasound (right) using 50, 100, 200 and 500 femtosecond laser pulses with the energy of 100 μJ.

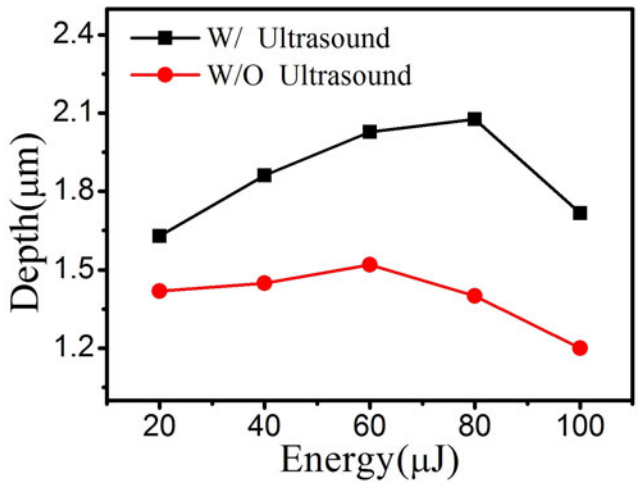

Fig. 8. The depth of holes drilled with 50 pulses versus laser energy, through the laser underwater machining with and without ultrasound assistance.

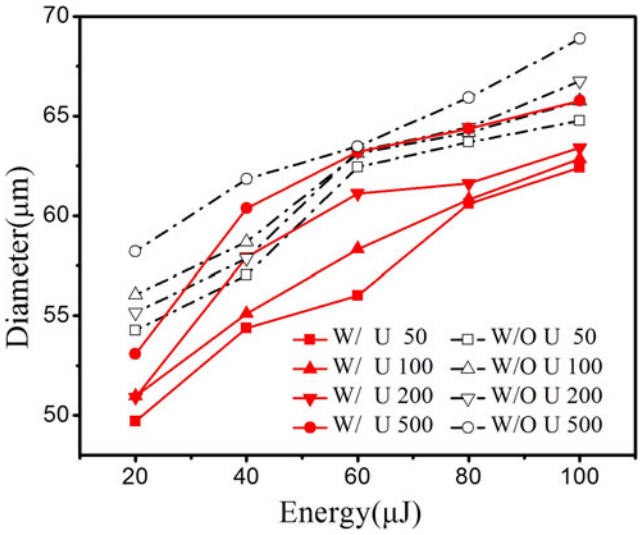

Fig. 9. The diameter of holes drilled with and without ultrasound, using four different pulse number versus laser pulse energy.

Meanwhile, crater morphology changed more regularly, smoothly and clearly. Moreover, ultrasound helps forming a clean and flat holes bottom. This method significantly improves the quality of femtosecond laser drilling underwater. In addition, the hole drilled with ultrasound assistance has a smaller orifice diameter,

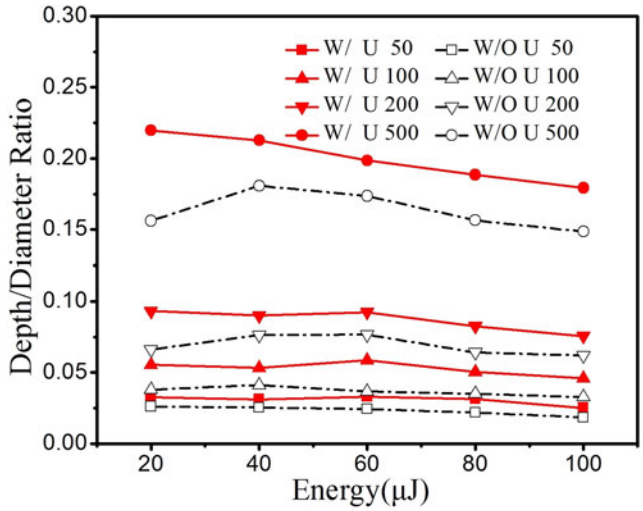

Fig. 10. The depth-to-diameter ratio of holes drilled with and without ultrasound using four different pulse number versus laser pulse energy.

deeper depth, and larger depth to diameter ratio about 20%. This suggests that the machining efficiency is improved, too.

Acknowledgements. This research work is supported by the National Key R&D Program of China (Grant Nos. 2017YFB1104800) and the National Natural Science Foundation of China (NSFC) (Grant Nos. 51875584, 51875585, 51475482, 51475481).

References

Abreu A, Levy-Bercowski D, Yu J, Salgueiro M, Kalathingal S and Susin LF (2005). Physical analyses of optical breakdown and plasma formation in water induced by laser. *Acta Photonica Sinica* **34**, 1610–1614.

Charee W, Tangwarodomnukun V and Dumkum C (2016) Ultrasonic-assisted underwater laser micromachining of silicon. *Journal of Materials Processing Technology* **231**, 209–220.

Chen X, Xu RQ, Chen JP, Shen ZH, Jian L and Ni XW (2004) Shock-wave propagation and cavitation bubble oscillation by ND:YAG laser ablation of a metal in water. *Applied Optics* **43**, 3251–3257.

Chichkov BN, Momma C, Nolte S, Alvensleben FV and Tünnermann A (1996) Femtosecond, picosecond and nanosecond laser ablation of solids. *Applied Physics A* **63**, 109–115.

Chien WT and Hou SC (2007). Investigating the recast layer formed during the laser trepan drilling of inconel 718 using the Taguchi method. *International Journal of Advanced Manufacturing Technology* **33**, 308–316.

Chu D, Sun X, Dong X, Yin K, Luo Z and Chen G (2017) Effect of double-pulse-laser polarization and time delay on laser-assisted etching of fused silica. *Journal of Physics D: Applied Physics* **50**, 465306.

Deng G, Su W, Duan J, Fan N, Sun X and Zhou J (2016). Research on ablation process of constant elastic alloy with femtosecond laser in solution medium. *Applied Physics A* **122**, 861.

Hu Y, Yue H, Duan J, Wang C and Zhou J (2017). Experimental research of laser-induced periodic surface structures in a typical liquid by a femtosecond laser. *Chinese Optics Letters* **15**, 54–58.

Juodkazis S, Okuno H, Kujime N, Matsuo S and Misawa H (2004). Hole drilling in stainless steel and silicon by femtosecond pulses at low pressure. *Applied Physics A* **79**, 1555–1559.

Kawata S, Sun HB, Tanaka T and Takada K (2001). Finer features for functional microdevices. *Nature* **412**, 697–698.

Lauterborn W and Bolle H (2006). Experimental investigations of cavitation-bubble collapse in the neighbourhood of a solid boundary. *Journal of Fluid Mechanics* **72**, 391–399.

https://doi.org/10.1017/S0263034618000538 Published online by Cambridge University Press

Liu H, Chen F, Wang X, Yang Q, Hao B and Si J (2012). Influence of liquid environments on femtosecond laser ablation of silicon. *Thin Solid Films* **518**, 5188–5194.

Liu Z, Wu B, Samanta A, Shen N, Ding H and Xu R (2016) Ultrasound-assisted water-confined laser micromachining (UWLM) of metals: experimental study and time-resolved observation. *Journal of Materials Processing Technology* **245**, 259–269.

Liu Z, Gao Y, Wu B, Shen N and Ding H (2014). Ultrasound-assisted water-confined laser micromachining: a novel machining process. *Manufacturing Letters* **2**, 87–90.

Matsumura T, Kazama A and Yagi T (2005). Generation of debris in the femtosecond laser machining of a silicon substrate. *Applied Physics A* **81**, 1393–1398.

Nguyen TTP, Tanabe R and Ito Y (2014). Effects of an absorptive coating on the dynamics of underwater laser-induced shock process. *Applied Physics A* **116**, 1109–1117.

Park JK, Yoon JW and Cho SH (2012). Vibration assisted femtosecond laser machining on metal. *Optics and Lasers in Engineering* **50**, 833–837.

Singh RK (1996). Transient plasma shielding effects during pulsed laser ablation of materials. *Journal of Electronic Materials* **25**, 125–129.

Sun X, Dong X, Hu Y, Li H and Chu D (2015) A robust high refractive index sensitivity fiber Mach-Zehnder interferometer fabricated by femtosecond laser machining and chemical etching. *Sensors and Actuators A: Physical* **230**, 111–116.

Tamura A, Sakka T, Fukami K and Ogata YH (2013). Dynamics of cavitation bubbles generated by multi-pulse laser irradiation of a solid target in water. *Applied Physics A: Materials Science and Processing* **112**, 209–213.

Tomko J, O'Malley SM, Trout C, Naddeo JJ, Jimenez R and Griepenburg JC (2017). Cavitation bubble dynamics and nanoparticle size distributions in laser ablation in liquids. *Colloids & Surfaces A: Physicochemical & Engineering Aspects* **522**, 368–372.

Vorobyev AY and Guo C (2007). Femtosecond laser structuring of titanium implants. *Applied Surface Science* **253**, 7272–7280.

Wang C, Chu D, Duan J, Zhou J, Yin K and Sun X (2017). Micro-channel etching characteristics enhancement by femtosecond laser processing high-temperature lattice in fused silica glass. *Chinese Optics Letters* **15**, 56–59.

Wu B (2014). Ultrasound-assisted water-confined laser micromachining. US Patent.

Yin K, Duan J, Wang C, Dong X, Song Y and Luo Z (2016). Micro torch assisted nanostructures' formation of nickel during femtosecond laser surface interactions. *Applied Physics Letters* **108**, 041914.

Yin K, Du H, Dong X, Wang C, Duan JA and He J (2017) A simple way to achieve bioinspired hybrid wettability surface with micro/nanopatterns for efficient fog collection. *Nanoscale* **9**, 14620–14626.

Zeng X, Mao XL, Greif R and Russo RE (2005). Experimental investigation of ablation efficiency and plasma expansion during femtosecond and nanosecond laser ablation of silicon. *Applied Physics A* **80**, 237–241.

Zeng K, Hu Y, Deng G, Sun X, Su W and Lu Y (2017) Investigation on eigenfrequency of a cylindrical shell resonator under resonator-top trimming methods. *Sensors* **17**, 2011.

Zhang D, Gökce B, Sommer S, Streubel R and Barcikowski S (2016) Debris-free rear-side picosecond laser ablation of thin germanium wafers in water with ethanol. *Applied Surface Science* **367**, 222–230.

Zhu J, Yin G, Zhao M, Chen D and Zhao L (2005). Evolution of silicon surface microstructures by picosecond and femtosecond laser irradiations. *Applied Surface Science* **245**, 102–108.

https://doi.org/10.1017/S0263034618000538 Published online by Cambridge University Press